

## An Application of High-Power Ultrasound to Rubber Recycling

Chang Kook Hong\* and A. I. Isayev\*\*

*\*Department of Chemical Engineering and Center for Composite Materials,  
University of Delaware, Newark, Delaware 19716, USA*

*\*\*Institute of Polymer Engineering, The University of Akron, Akron, OH 44325, USA*

(Received June 5, 2003, Accepted June 9, 2003)

**ABSTRACT** : The application of powerful ultrasound to rubber recycling is a very recent field of study. An ultrasonic field creates high frequency extension-contraction stresses by acoustic cavitation. The breakdown of rubber network occurs primarily around pulsating cavities due to the highest level of strain produced by high-power ultrasound. Stronger reductions of cross-link density were observed at a higher pressure, indicating an important role of pressure during ultrasonic recycling. Visible bubbles were observed during ultrasonic treatment as a proof of acoustic cavitation. Shearing effect has a significant influence on improving the efficiency of ultrasonic treatment. After the ultrasonic treatment, the cross-link densities of NR/SBR blends were lower than those of NR and SBR due to the reduced degree of unsaturation and chemical reactions. Carbon black fillers increase the probability of bond scission during ultrasonic treatment, due to the restricted mobility. The mechanical properties of ground tire rubber (GRT)/HDPE blends were improved by ultrasonic treatment and dynamic re-vulcanization. Ultrasonic treatment of GRT in the presence of HDPE matrix was found to give better mechanical properties due to the chemical reactions between rubber and plastic phases.

*Keywords* : rubber recycle, ultrasound, NR/SBR blend, Ground tire rubber/HDPE blend.

### I . Introductio

The environmental problems created by discarded tires and waste rubbers have been significant in recent years. The management of waste rubbers has also become a growing problem in rubber industry. The large and rapidly growing accumulation of piles of scrap tires and waste rubbers causes fire and health hazards, and environmental problems.<sup>1</sup> Increasing legislation restricting the disposal of used tires and waste rubber has demanded the search for economical and environmentally sound methods of recycling.

The cross-linked elastomers are solid, insoluble and infusible. The presence of a three-dimensional crosslinked network creates tremendous problems in rubber recycling. A number of methods<sup>2-5</sup> have been

applied in attempt to solve the problem and to find more effective ways of rubber recycling. However, they are either uneconomical or are not sufficient to represent a complete solution. Recently, a novel patented continuous process has been developed for recycling of waste rubbers as a suitable way to recycle a ground tire rubber,<sup>6-8</sup> unfilled NR,<sup>9</sup> SBR,<sup>10-16</sup> EPDM,<sup>17</sup> silicon rubber<sup>18-21</sup> and polyurethane rubber.<sup>22</sup> This technology is based on the use of the high power ultrasound. The ultrasonic waves of certain levels in the presence of pressure and heat can break up the three-dimensional network in crosslinked rubber. The ultrasonically treated rubber can be reprocessed, shaped and re-vulcanized in very much the same way as the virgin rubber. The process of ultrasonic devulcanization is very fast and occurs on the order of a second and may lead to

the preferential breakage of sulphidic cross-links in vulcanized rubbers. Devulcanization in sulfur-cured rubber can be defined as the process of cleaving, totally or partially, poly-, di- and mono-sulfidic crosslinks that are formed during the initial vulcanization.<sup>23</sup>

The proposed ultrasonic devulcanization model<sup>24</sup> was based upon a mechanism of rubber network breakdown caused by acoustic cavitation. It is well known that some amounts of cavities or small bubbles are present in rubber during any type of rubber processing.<sup>25</sup> Moreover, the formation of visible bubbles can be nucleated by precursor cavities of appropriate size.<sup>26,27</sup> Driven by ultrasound, the cavities pulsate with amplitude depending mostly upon the difference between ambient and ultrasonic pressures (acoustic cavitation). The devulcanization of rubber network can occur primarily around pulsating cavities due to the highest level of strain produced by the powerful ultrasound.<sup>28</sup> In contrast to plastics, rubber chains break down only when they are fully stretched.<sup>29,30</sup> An ultrasonic field creates high frequency extension-contraction stresses in crosslinked viscoelastic media. The effects of rubber viscoelasticity have been considered in the description of dynamics of cavitation.<sup>28,31</sup> Also, the shearing effect during the ultrasonic treatment should be considered.

The main objective of this research is to enhance our understanding of the ultrasonic recycling of rubbers. The basic goals of this study are: (1) to study the effect of pressure and shearing on ultrasonic process, (2) to investigate the similarities and differences in the devulcanization behavior of natural, synthetic rubber and their blends, (3) to understand the effect of fillers on ultrasonic treatment, and (4) to perform comprehensive studies of blending ultrasonically treated waste rubber with thermoplastics.

**Table 1. The compounding ingredients.**

Material	Name	Supplier
Zinc Oxide	ZnO	Akrochem Corp
Stearic Acid		Akrochem Corp
Sulfur	Rubber grade	Akrochem Corp
Accelerator	CBS <sup>a</sup>	Monsanto Inc.
	TBBS <sup>b</sup>	Monsanto Inc.
Carbon Black	HAF, N330	Huber Engineered Carbons

<sup>a</sup> CBS: N-cyclohexylbenzothiazole-2-sulfenamide

<sup>b</sup> TBBS: N-tert-butyl-2-benzothiazole sulfenamide

## II. Experimental

### 1. Materials

Natural rubber (SMR CV 60, Akrochem) and styrene-butadiene rubber (Duradene 706, Firestone Co.) were used in the experiments. The molecular weight ( $M_n$ ) of SBR is  $1.07 \times 10^5$  g/mole and polydispersity index is 3.63. The ground tire rubber (GRT) obtained from Rondy Inc. was also used. The GRT was 10-mesh ground rubber from the treads and sidewalls of passenger and truck tires. Polyethylene used was high-density polyethylene (HDPE, Marlex HMN4550-3) having melt flow index (MFI) of 4.8 from Phillips Chemical Company. The other compounding ingredients are summarized in Table 1.

### 2. Static Ultrasonic Treatment of SBR

The recipe used was 1 phr Sulfur and 1.3 phr CBS. The compression molding of sheets ( $230 \times 114 \times 2$  mm<sup>3</sup>) was performed using an electrically heated compression molding press (Wabash) at 175°C. The molded sheets were cut using an arch-punch of 25.4 mm diameter. Also, in order to investigate the effect of the concentration of cavities on ultrasonic treatment, the vulcanized samples were ground using Nelmor grinding machine (model Q1012M1). The average particle diameter was about 0.711 mm (28 mesh). The ground sample was com

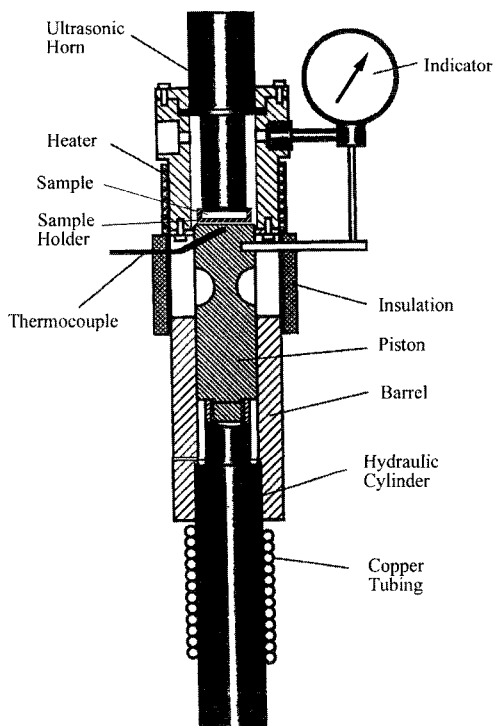


Figure 1. Schematic of static ultrasonic device.

pressed in a cylinder-type mold (diameter of 25.4 mm and thickness of 2 mm) at 100°C to make the same shape as the sheet sample.

Static ultrasonic treatment was carried out by static ultrasonic device (Figure 1) at 120°C. The prepared samples were put into a sample holder to prevent leakage under pressure. The horn diameter was 25.4 mm. The ultrasonic amplitude, the pressure in the gap, and the exposure time to the ultrasound were varied.

### 3. Continuous Ultrasonic Treatment of Filled NR and NR/SBR Blends

Carbon black (CB) filled NR compounds were mixed using a water-cooled Banbury mixer (Farrel) and a two-roll mill (Dependable Rubber Machinery Co.). The recipes used in this study are given in Table 2. The NR/SBR blends were prepared on a two-roll mill at 50°C according to ASTM D15-627.

Table 2. Recipes for NR compounds.

Comp.	NR	Sulfur	CBS	ZnO	Stearic Acid	CB
Recipe 1	100 (virgin)	2	1	5	1	0-60
Recipe 2	100 (devulcanized)	2	0	2.5	0.5	0-60
Recipe 3	100 (devulcanized)	2	0.5	2.5	0.5	0-60

Unit: phr

Table 3. Recipes for NR/SBR blends.

Comp.	NR/SBR	Sulfur	CBS	ZnO	Stearic Acid
Recipe 1	100 (virgin)	2	1.1	5	1
Recipe 2	100 (devulcanized)	2	0	5	1

Unit: phr

The compounding recipe is given in Table 3. The compression molding was performed at 160°C. According to the cure curve, the optimum cure time was determined. After molding, the vulcanized samples were ground using a grinding machine.

Continuous ultrasonic treatment was carried out using an extruder with an ultrasonic die attachment, shown in Figure 2. The temperature of the extruder barrel was set at 120°C. The gaps between the die and horn were set at 1.52, 2.03 and 2.54 mm. The flow rates were 0.63, 1.26 and 2.52 g/s. The rubber exiting the die was devulcanized in the gap between the ultrasonic horn and die plate at amplitudes of 5, 7.5, 10  $\mu\text{m}$ . The devulcanized rubber was water-quenched and air-dried.

The devulcanized rubber was compounded with curatives on the two-roll mill. Revulcanization was then carried out in the compression molding press. Different revulcanization recipes were used in order to enhance the mechanical properties of the devulcanized NR on revulcanization as shown in Table 2. The devulcanized NR/SBR blends were com

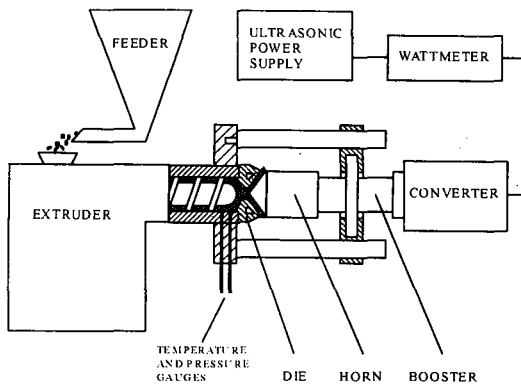


**Figure 2.** Schematic of the continuous reactor with coaxial ultrasonic die attachment.

pounded with curatives according to the recipe used for the virgin compound.

#### 4. HDPE/GRT Blends Using Ultrasonic Treatment

The GRT was devulcanized in the continuous ultrasonic extruder. The temperature of the extruder barrel was set at 178°C. GRT was then fed into the extruder at a flow rate of 2.77 g/s. The gap between the horn and the die was set at 2 mm. The amplitude of ultrasound was 10  $\mu\text{m}$ . Table 4 shows the results of gel fraction and crosslink density of GRT, devulcanized GRT (DGRT) and revulcanized GRT (RGRT).

HDPE/RGRT blends of various concentrations were prepared by using a laboratory internal mixer (PL-2000, C. W. Brabender). To prepare the blend, HDPE was first added into the mixer for about two minutes at 150°C. After HDPE was melted, DGRT was mixed with the molten HDPE. When the torque

**Table 4.** Gel fraction and crosslink density.

	Gel Fraction(%)	Crosslink Density ( $\text{kmol}/\text{m}^3 \cdot 10^2$ )
GRT	82.4	9.75
DGRT	70.6	3.01
RGRT	83.6	11.71

reached a steady state value, curatives (1 phr Sulfur and 1 phr TBBS) were added into the mixer for dynamic revulcanization. The torque generally increases due to the cross-linking reaction and then levels off. Total time for the blending was 11 minutes. The same mixing procedure was applied for HDPE/GRT, HDPE/DGRT blends, but no curatives were added.

Also, a co-rotating twin-screw extruder (JSW Labotex30) was used to mix HDPE with GRT prior to devulcanization. HDPE and GRT were physically mixed and then fed to the extruder. Feeding rate was 50 g/min. Screw speed was set at 150 rpm and zone temperatures of 140°C/140°C/145°C/150°C/150°C/155°C/160°C were used. After drying, HDPE/GRT blends were passed through the ultrasonic extruder, operated at the same conditions as in the case of devulcanization of GRT described earlier. The dynamic revulcanization of the HDPE/DGRT blends was carried out in an internal mixer. The compressing molding was performed at a temperature of 160°C for 5 minutes. The samples were cooled in water under compression to maintain the overall dimensional stability and flatness of the sheets.

#### 5. Characterization

A Monsanto oscillating disc rheometer was used to obtain the torque-time curves according to ASTM D2084.

The gel fractions of the samples were measured by the Soxhlet extraction methods using benzene for NR and SBR, and 1,1,1-trichloroethane for GRT as solvent. The cross-link densities were characterized by the swelling method using the Flory-Rehner equation.<sup>32,33</sup> In carbon black filled system, the Flory-Rehner equation has to be modified using the Kraus correction.<sup>34</sup>

The rheological behavior was investigated using a Monsanto Processability Tester (MPT) according to ASTM D5099. End corrections were applied for the calculations of the shear viscosity.

An Instron tensile tester (model 5567) was used

for the mechanical property measurements. All tests were performed at room temperature with a crosshead speed of 500 mm/min.

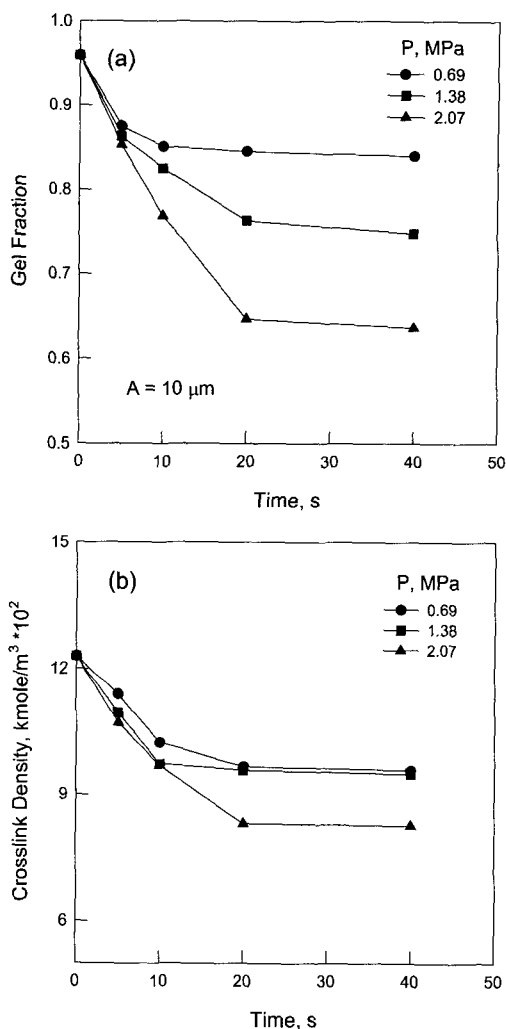
A Hitachi S-2150 Scanning Electron Microscope (SEM) was used to characterize the morphology of plastic/rubber blends. The samples are coated with gold using sputter coater.

### III. Results and discussion

#### 1. The Effect of Pressure and Shearing on Ultrasonic Process

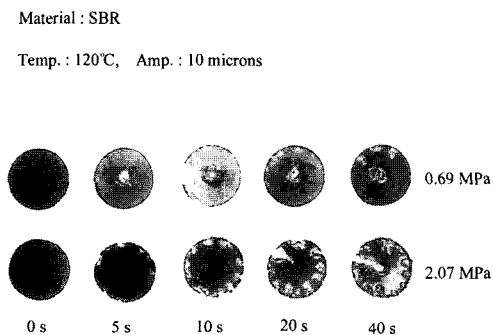
A static ultrasonic treatment device was used to investigate the effect of pressure and shearing on ultrasonic treatment. The gel fraction and cross-link density of statically treated samples at various initial pressures are shown in Figure 3. The gel fraction and cross-link density was significantly decreased with increase in pressure. This observation is explained as that the ultrasonic (acoustic) pressure in the rubber layer increases with increase in ambient pressure.<sup>28</sup> Typically, both acoustic pressure and ultrasonic power consumption increase at high static pressure and low gap clearance. Under these conditions, transient acoustic cavitation proceeds and the breakdown of the network can take place more effectively as observed in experiments. However, as the exposure time was increased, the gel fraction and cross-link density leveled off. The reason for the leveling off is some decay of the pressure caused by squeezing out of some amount of rubber sol. The latter led to a decrease of power consumption during static ultrasonic treatment. Therefore, decreasing the pressure caused the lowering of ultrasonic efficiency.

Figure 4 shows the photographs of statically treated SBR disks by ultrasound at different pressures and times. Some visible bubbles are observed at the center of the samples at low pressure and at the edges at high pressure after 5 s. At longer exposure times the bubble are generated at both edges and centers of the samples. Evidently, the pulsating cavities created by ultrasound waves break



**Figure 3.** Gel fraction (a) cross-link density (b) vs. ultrasonic exposure time for statically treated SBR disks at various pressures.

the cross-links and chemical bonds in rubber, which in turn create visible bubbles. In fact, the rubber sol generated during the treatment is mainly localized in the area where bubbles are present. The localized effect<sup>35</sup> of ultrasonic waves along with pressure at the edges caused the localized bubbles. These observations are clear indications of the existence of cavitation in the rubber during the ultrasonic devulcanization.<sup>36</sup> The cavitation usually corresponds to the effect of formation and growth



**Figure 4.** Photographs of statically treated SBR disks by ultrasound at pressures of 0.69 and 2.07 MPa and various exposure times.

of voids in gas-saturated rubber samples after sudden depressurization.<sup>26,27</sup> It is also seen from Figure 4 that greater degradation took place at higher pressure. Therefore, the pressure has a significant effect on improving the efficiency of ultrasonic devulcanization of rubber.

In order to investigate the effect of the concentration of voids (cavities) on ultrasonic treatment, disks prepared from ground SBR particles were subjected to ultrasonic treatment. Clearly, the disks from the ground particles have a higher concentration of voids than the sheet disks. The gel fraction and cross-link density of devulcanized rubbers obtained from ground and sheet samples is presented in Figure 5. The gel fraction and cross-link density of the devulcanized ground samples are lower than those of sheet samples. An ultrasonic field creates high frequency expansion-contraction stresses on voids. The pulsating voids can break the cross-links and chemical bonds in rubber. Therefore, the ground sample, having a higher concentration of voids, is affected more by ultrasonic cavitation than the sheet sample.

The comparison of static (without shear) and continuous (with shear) process was made to investigate if the presence of shearing has any effect on ultrasonic devulcanization. Figure 6 shows a com

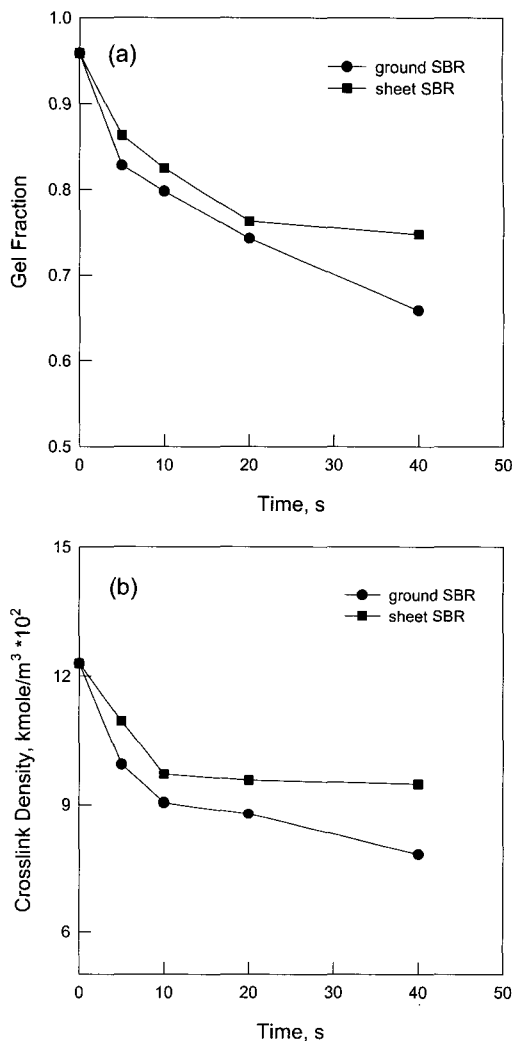


**Figure 5.** Gel fraction (a) cross-link density (b) vs. exposure time for SBR disks made of ground particles and from sheets, statically treated at 10  $\mu\text{m}$ , 1.38 MPa and 12 0°C.

parison of gel fraction and cross-link density of devulcanized rubber samples obtained in static and continuous experiments. The gel fraction and cross-link density of continuously devulcanized samples are consistently lower than those of the statically devulcanized samples. In particular, Figure 6(b) indicates that the presence of shearing and high pressure in continuous process has a strong effect on reducing cross-link density. However, this com

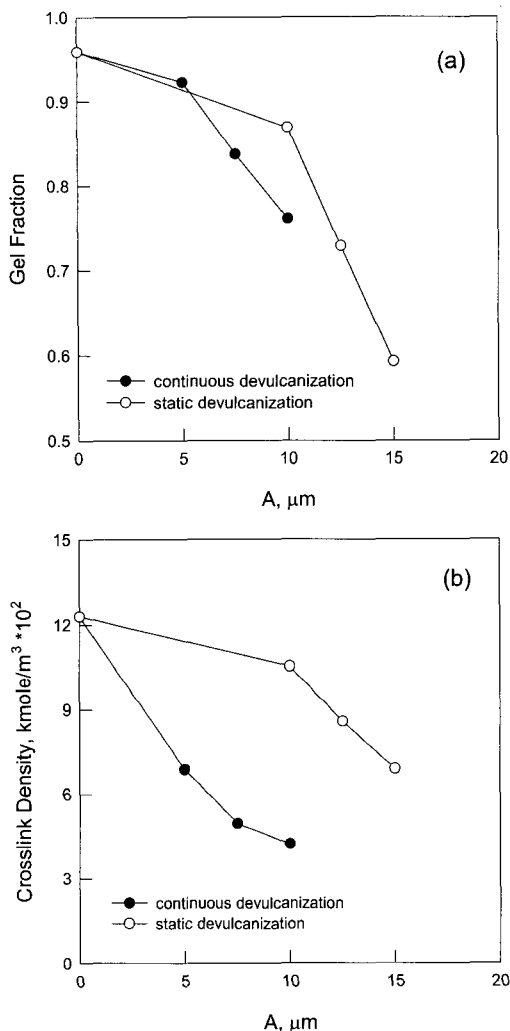


**Figure 6.** Gel fraction (a) crosslink density (b) vs. ultrasonic amplitude for statically and continuously devulcanized ground SBR.

parison of static and continuous devulcanization does not clearly answer the question concerning what effect the shearing has on devulcanization.

Figure 7 presents normalized gel fraction as a function of normalized cross-link density in the gel of statically and continuously<sup>16</sup> devulcanized samples. For each process, the dependence of gel fraction on cross-link density is described by a unique curve independent of processing conditions such as pressure, temperature and amplitude. The

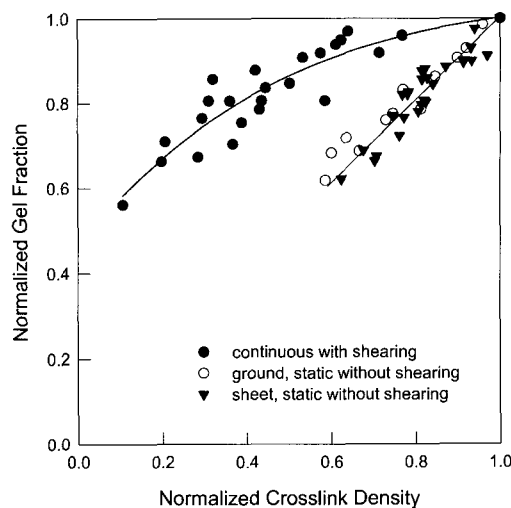


**Figure 7.** Normalized gel fraction vs. normalized crosslink density in the gel of statically and continuously treated unfilled SBR obtained at different processing conditions.

unique correlation between gel fraction and cross-link density observed in the continuous process is shifted toward higher values of cross-link density in the static experiments. Therefore, the shearing effect has a significant influence on improving the efficiency of ultrasonic devulcanization as evident from significant reduction in cross-link density in the continuous process.

## 2. A Model of Bubble Formation by Acoustic Depressurization

Cavitation is the process of bubble formation by pressure reduction. The reduction of pressure may be effected by mechanical means, placing the material under tension, or by acoustic means, where rarefaction waves similarly introduce negative pressure.<sup>37</sup> The cavitation in rubbers usually corresponds to the effect of formation and unrestricted growth of voids in gas-saturated rubber samples after a sudden depressurization.<sup>26,27</sup> The formation and growth of the bubbles play an important role in the devulcanization of rubbers by ultrasound.

Consider gas-saturated samples under pressure  $P_s$  at temperature  $T$  (state I) as a thermodynamic

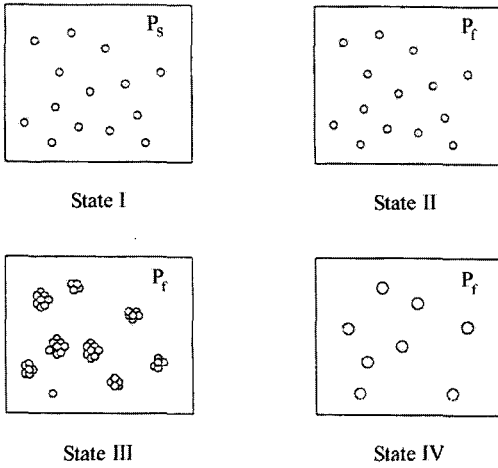


**Figure 8.** Bubble formation process by a pressure reduction ( $P_s > P_f$ ).

system of equilibrium. As a result of a pressure reduction to the pressure  $P_f$ , the dissolved gases become supersaturated (state II). In this supersaturation state, aggregation of the dissolved gas molecules into clusters may be imagined (state III). After the cluster state, bubbles can be formed (state IV). This approach<sup>38</sup> deals with aggregates of dissolved gas molecules. These four states experienced by the dissolved gas molecules due to a pressure reduction are shown in Figure 8.

The change in free energy of the cluster with dissolved gas molecules plus the surface energy is the free energy,  $F_n$ , required to form a cluster,<sup>38</sup>

$$F_n = (P_f - P_s)n\nu_m + \frac{3}{2}kTn^{2/3} \tag{1}$$

where  $\nu_m$  is the volume of a dissolved gas molecule and  $k$  is Boltzmann constant. The condition for a minimum with respect to in the free energy of formation is

$$(P_s - P_f)n^{1/3} = \frac{kT}{\nu_m} \tag{2}$$

When a cluster meets the stability condition, the

cluster spontaneously expands and attains enough space for the bubble. The difference of chemical potentials of state I and IV is

$$kT \ln(P_g / P_s) = -\nu_m(P_s - P_f) \tag{3}$$

Equation (3) determines the pressure inside a bubble,  $P_g$  after the expansion. The corresponding volume may be obtained from the ideal gas equation

$$P_g V_g = nkT \tag{4}$$

Since  $nkT = const.$  during this expansion process, the free energy is also invariant.

$$F_{n,cluster} = F_{n,bubble} \tag{5}$$

It is known that the effective volume of the dissolved gas molecules depends on the materials. The translation kinetic energy is partially restrained by the material. Therefore, a parameter called the lost degrees of freedom ( $f_L$ ) is introduced as the gas dissolves in the material.<sup>38</sup>

$$\frac{f_L}{3} = \frac{\nu_m}{\nu_e} \tag{6}$$

where  $\nu_e$  is the effective volume of the dissolved gas molecule. For example, if the volume of the dissolved gas molecule is the pure equilibrium volume, its lost degree of freedom is 3. Therefore, the free energy needed to form a cluster is modified as follows:

$$F_n = (P_f - P_s)n\nu_e + \frac{f_L}{2}kTn^{2/3} \tag{7}$$

The rate of formation of bubbles per unit time per unit volume  $J$  (i.e. the number of bubbles formed per second per cubic meter) can be obtained from a classical nucleation theory. The nucleation rate in polymer solution is given by<sup>39,40</sup>:



$$J_n = N_g B \exp\left(-\frac{F_n}{kT}\right) \quad (8)$$

where  $N_g$  is the number of gas molecules dissolved per unit volume and  $B$  is the frequency factor. The frequency factor  $B$  in equation (8) represents the frequency that gas molecules impinge upon the embryo nucleus. Generally, the frequency factor  $B$  is considered as an adjustable parameter due to a lack of experimental data for evaluating it correctly.<sup>39</sup>

The acoustic pressure ( $P_A$ ) in a bulk material is calculated by the simplified formula<sup>41</sup>

$$P_A = \rho \omega c A \quad (9)$$

where  $\rho$  is the density of the polymer,  $\omega$  is the angular frequency of ultrasound,  $c$  is the velocity of the sound in polymer and  $A$  is the ultrasonic amplitude. However, this case is different from the situation that occurs during ultrasonic devulcanization. Yashin and Isayev<sup>31</sup> considered the problem of calculating ultrasonic pressure for such a case employing the methods of linear acoustics. The one-dimensional problem was considered in which all-ultrasonic waves propagate parallel to the z-axis and normally to the rubber (thickness of  $h$ )-metal interface. The acoustic pressure ( $P_A$ ) is calculated by the following formula<sup>31</sup>

$$P_A(z) = -\rho \omega c A \operatorname{Re} \left[ \frac{i}{1+i \frac{\tan \delta}{2}} \frac{(Z_n + Z_r) \exp(iq(z-h)) + (Z_n - Z_r) \exp(iq(h-z))}{(Z_n + Z_r) \exp(iqh) - (Z_n - Z_r) \exp(iqh)} \right] \quad (10)$$

where  $q$  is the wave number of ultrasound in rubber.

$$q = \frac{\omega}{c} \left( 1 + i \frac{\tan \delta}{2} \right) \quad (11)$$

It includes the imaginary part describing absorption of sound in rubber. Here  $Z_m$  and  $Z_r$  are the acoustic impedances of the metal and rubber part.

$$Z_m = \rho_m c_m \quad (12)$$

$$Z_r = \frac{\rho c}{1 + i \frac{\tan \delta}{2}} \quad (13)$$

This facilitates estimating the effects of processing conditions, i.e., gap clearance and ambient pressure, on acoustic pressure and therefore on cavitation.

The numerical calculations were performed for the case of gas-saturated sample that has a large amount of dissolved gas molecules. The formation of bubbles depends on pressure difference (depressurization) between ambient and acoustic pressures. The rate of bubble formation ( $J_n$ ) and the initial radius of a bubble ( $R_o$ ) were calculated in the case of one depressurization by ultrasound of frequency 20 kHz and amplitude 10  $\mu\text{m}$  in static condition. The parameters used in this study are collected in Table 5.

Figure 9 shows the effect of number of dissolved gas molecules in the sample on nucleation rate. The dissolved gas in the rubber is the nuclei for bubble

**Table 5. The parameters used in numerical calculations.**

Symbol	Description	Data
$P_D$	Die pressure	1.38 MPa
$P_s$	Ambient pressure	0.110 MPa
$h$	Sample thickness	1.52 mm
T	Temperature of die	393 K
$\sigma_{LJ}$	Lennard-Jones parameter of $N_2$	$3.86 \times 10^{-10} \text{ m}^{42}$
$\nu_m$	The volume of a dissolved gas	$(2^{0.5}/6) \times \sigma_{LJ}^3$ <sup>42</sup>
$n_g$	The No. of dissolved gas molecules	$6.022 \times 10^{23} \text{ No./m}^3$
$f_L$	The lost degree of freedom	1.40
$B$	A frequency factor	$\text{Exp}(1)^{0.5}$ <sup>38</sup>
$\rho$	Density of SBR	$933 \text{ kg/m}^3$ <sup>43</sup>
$\tan \delta$	Loss tangent	0.5
$c$	Bulk sound velocity	$1485 \text{ m/s}$ <sup>43</sup>
$c_m$	Sound velocity in steel	$5790 \text{ m/s}$ <sup>41</sup>
$\rho_m$	Density of steel	$7900 \text{ kg/m}^3$

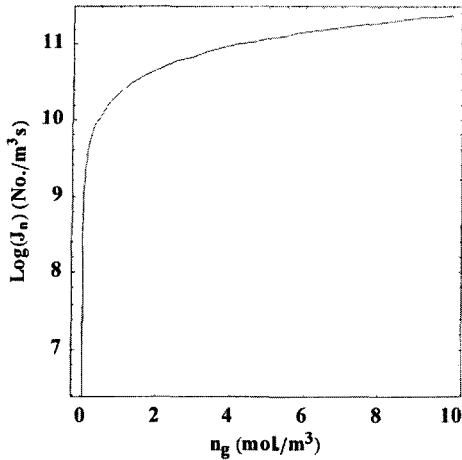


Figure 9. The effect of number of dissolved gas molecules on the rate of bubble formation.

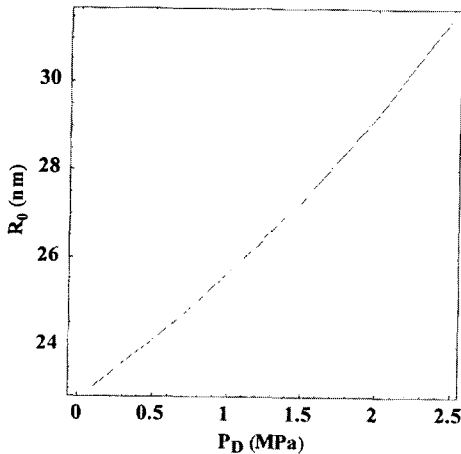


Figure 10. The initial radius of bubble as a function of die pressure.

formation and can aggregate and form bubbles during a depressurization process by ultrasound. Therefore, the number is an important parameter in this calculation. As shown in Figure 9, the rate of bubble formation increases with increasing initial number of dissolved gas molecules.

Figures 10 shows the initial radius of bubble as a function of die pressure. The initial radius increased with increase in die pressure. The effect of negative ultrasonic pressure is based on the diffe-

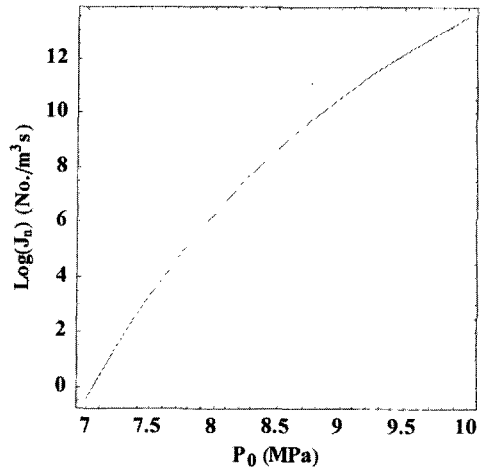


Figure 11. The rate of bubble formation as a function of acoustic pressure.

rence between die pressure and ultrasonic pressure. Therefore, as the die pressure increases and the initial radius of formed bubble increases. It was also reported<sup>31</sup> that ultrasonic pressure in the rubber layer increased with ambient pressure, which could be attributed to restoration of the bulk velocity of sound upon rubber compression. Therefore, if one considers network degradation around pulsating cavities by ultrasound, the effect of inflation of cavities increases with increase in die pressure. Figure 11 gives the rate of bubble formation as a function of acoustic pressure. The rate of bubble formation increases as acoustic pressure increases due to increased depressurization effect.

In this numerical calculation, the rate of bubble formation and the initial radius of bubble were considered upon a depressurization by ultrasound. Calculation of bubble growth by ultrasound and comparison with experimental data are remained for next work.<sup>28,31</sup> Also, viscoelastic properties of rubber and dynamics of cavitation during bubble formation should be considered.

### 3. Ultrasonic Treatment of NR/SBR Blends

The objectives of this study are to understand the ultrasonic treatment of NR/SBR blends in which two

networks of different natures are present, and to investigate the similarities and differences in the devulcanization behavior of NR, SBR and their blends. The use of blends of rubbers is almost as old as the synthetic rubber industry and generally stems from an understandable desire to combine the best features - technical or economic - of two rubbers.<sup>44</sup>

The cure curves using recipe 2 in Table 3 for devulcanized NR/SBR blend of 50/50 obtained at different ultrasonic amplitudes are seen in Figure 12. The maximum torque, which relates to cross-link density, of devulcanized NR/SBR blend (50/50) is lower than that of the virgin sample. During the ultrasonic devulcanization of the blends along with the breakup of cross-links, a possibility exists for breakup of main chains.<sup>45</sup> The maximum torque of devulcanized NR/SBR blend of 50/50 shows a minimum at 7.5  $\mu\text{m}$ . As shown in Figure 12, the cure behavior of virgin and devulcanized blend is significantly different. The shortness or almost absence of the scorch time in devulcanized sample indicates that the cross-linking reactions may start immediately upon heating.<sup>14,45</sup>

Figure 13 gives the ultrasonic power consumption during devulcanization of cured NR, SBR and NR/SBR blends. Similar to pure NR, the ultrasonic power consumption for the NR/SBR blends of 75/25, 50/50 passed through a maximum at 7.5  $\mu\text{m}$ . The reason is due to the competition between bond breakage and reformation during ultrasonic devulcanization. While devulcanization is dominant in between 5 and 7.5  $\mu\text{m}$ , some reactions between the broken bonds occur with increasing intensity when the ultrasound amplitude is increased from 7.5 to 10  $\mu\text{m}$ , which accounts for the reduction in power consumption at 10  $\mu\text{m}$ .<sup>9</sup> For pure SBR and the blend of 25/75, the power consumption increased with increasing ultrasonic amplitude. In this case, the higher the ultrasonic amplitude, the more the devulcanization, and more power is needed to carry it out. In the blends of 75/25 and 50/50, NR contributes more to devulcanization of the blends, and

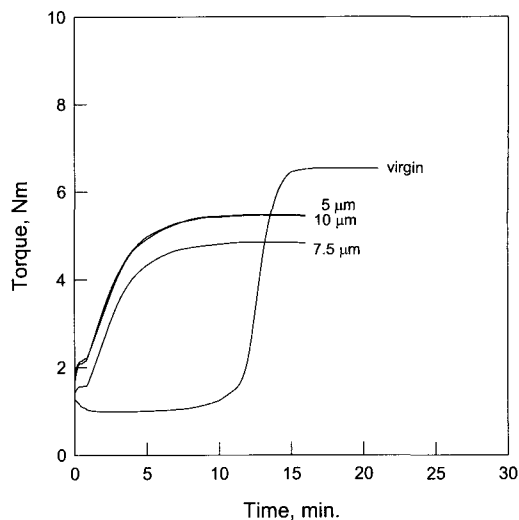


**Figure 12.** Cure curves for virgin and ultrasonically devulcanized NR/SBR blend of 50/50wt. %.

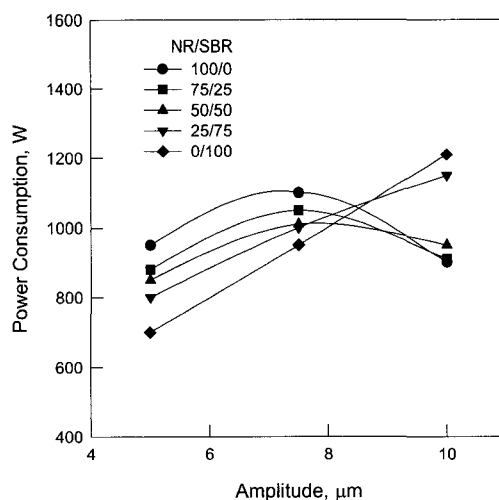


**Figure 13.** Ultrasonic power consumption as a function of ultrasonic amplitude during devulcanization of cured NR, SBR and NR/SBR blends.

in the blend of 25/75, SBR contributes more to the devulcanization. The power consumption of NR is higher than that of SBR from 5  $\mu\text{m}$  to 7.5  $\mu\text{m}$ . The higher power consumption leads to a higher degree of devulcanization. Therefore, NR is easier to devulcanize than SBR.<sup>46</sup> The differences in devul

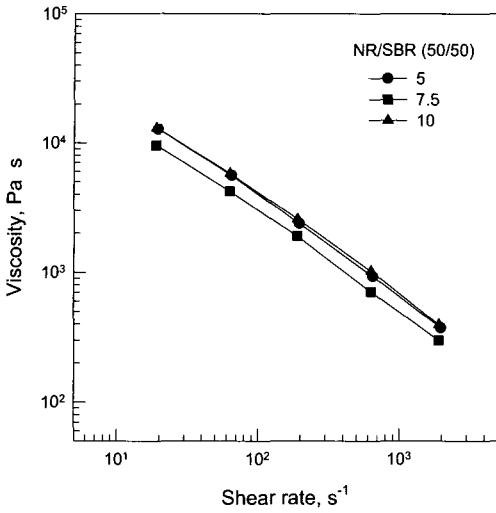


Figure 14. Flow curves of ultrasonically devulcanized NR/SBR blend of 50/50wt. % at various amplitudes.

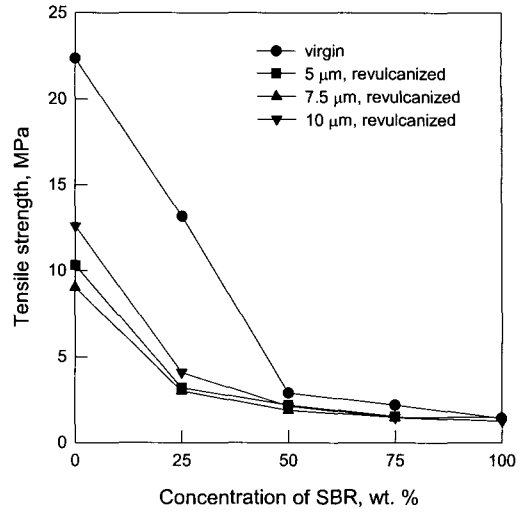


Figure 16. Tensile strength of virgin vulcanized and revulcanized NR/SBR blends.

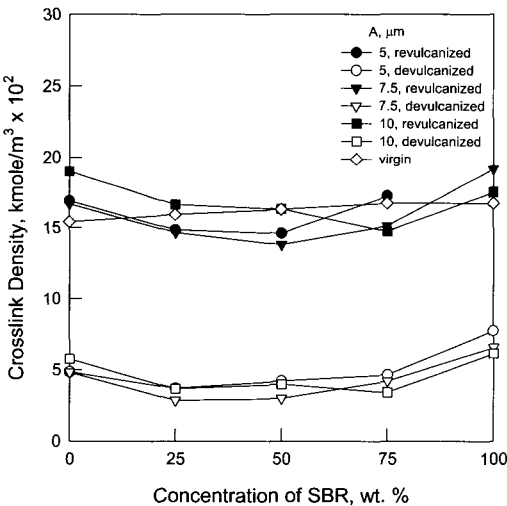


Figure 15. Cross-link density of virgin vulcanized, devulcanized and revulcanized NR/SBR blends as a function of concentration of SBR.

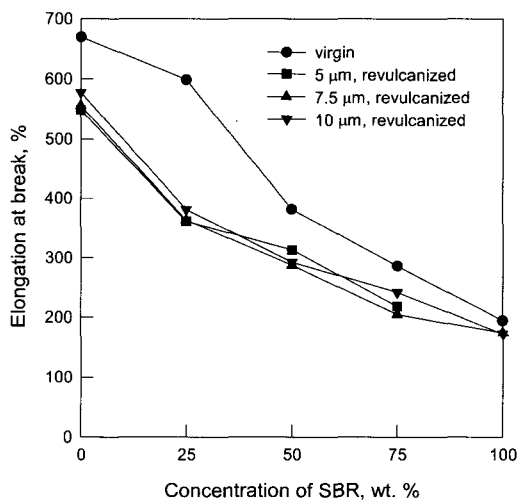


Figure 17. Elongation at break of virgin vulcanized and revulcanized NR/SBR blends.

canization between NR and SBR would be due to the different structure of the polymer chain and/or thermal properties.

Figure 14 gives the flow curves of devulcanized NR/SBR blends of 50/50 at various amplitudes. The viscosity at 7.5  $\mu\text{m}$  is lower than the viscosity at

5 and 10  $\mu\text{m}$ . This observation is in accord with the ultrasonic power consumption shown in Figure 13, indicating higher power consumption at 7.5  $\mu\text{m}$ . It is clear that the higher power consumption leads to a higher degree of devulcanization and lower viscosity.

The cross-link density of virgin vulcanized,

devulcanized and revulcanized NR, SBR and the blends is shown in Figure 15. The cross-link densities of the devulcanized and revulcanized NR/SBR blends are lower than those of the devulcanized pure NR and SBR. It seems that the degree of unsaturation in the blends is decreased during ultrasonic treatment. Also, some reactions between networks of NR and SBR had occurred during ultrasonic treatment.<sup>47</sup>

Figures 16 and 17 give, respectively, tensile strength and elongation at break of virgin vulcanized and revulcanized blends as a function of concentration of SBR. The tensile properties of the blends increase with increasing NR content. However, the tensile strength and elongation at break of the revulcanized blends are lower than those of the virgin vulcanized blends. The deterioration in tensile properties of the revulcanized sample may be mainly due to main chain scission and remained networks during ultrasonic devulcanization.

#### 4. The Effect of Filler on Ultrasonic Treatment

The effect of filler on ultrasonic devulcanization of NR was investigated. The most common filler used for strengthening or reinforcing rubber is carbon black (CB). Due to the interaction between rubber and carbon black, the rubber molecules can be adsorbed onto the filler surface either chemically or physically.<sup>48</sup> Figure 18 shows the ultrasonic power consumption as a function of the carbon black loading at various amplitudes. On increasing CB content from 0 to 25 phr, power consumption shows a maximum at 7.5  $\mu\text{m}$ . The reason has been explained earlier<sup>9</sup> and is due to the competition between bond breakage and reformation during ultrasonic treatment. However, as CB content increases, CB may act as a radical acceptor of a special polyfunctional type.<sup>49</sup> If combination of polymeric radicals and CB occurs, then the reformation of broken bonds can be hindered. It is clear that higher power consumption leads to a higher degree of devulcanization as indicated by Figure 19 indicating gel

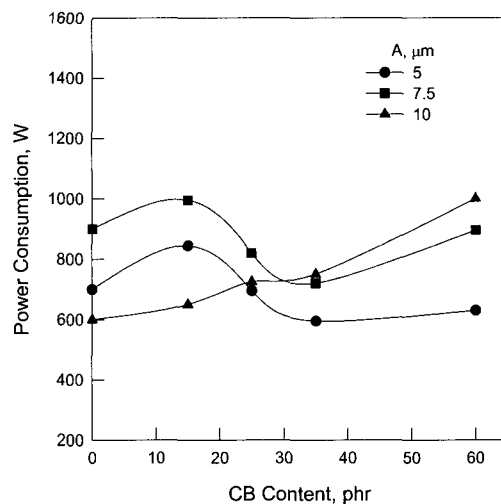


Figure 18. Ultrasonic power consumption during the devulcanization at various amplitudes.

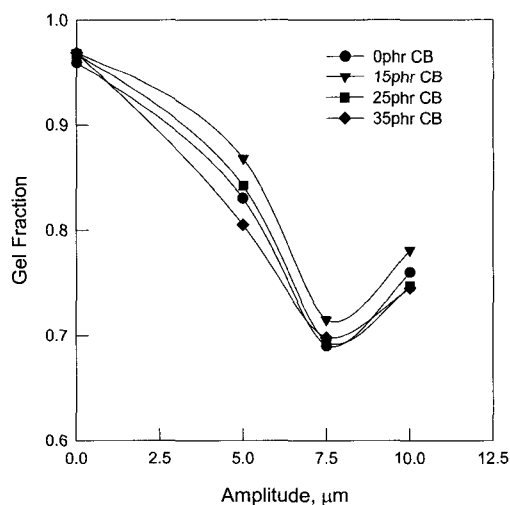


Figure 19. Gel fraction of devulcanized NR as a function of ultrasonic amplitude at various CB contents.

fraction of devulcanized unfilled and CB filled NR. The ultrasonic devulcanization of unfilled and CB filled NR indicates a minimum of gel fraction at intermediate amplitude that is independent of CB content. Due to the predominant effect of revulcanization from 7.5 to 10  $\mu\text{m}$ , the gel fraction increases. Also, the increase of the concentration of CB in NR leads to more devulcanization. Carbon

black fillers increase the probability of bond scission during ultrasonic treatment.

### 5. Blends of Ultrasonically treated GRT with HDPE

The blending devulcanized GRT with HDPE was considered using an internal mixer and a twin-screw extruder. This study is directed to improvement of the blending process and mechanical properties by dynamic revulcanization of devulcanized GRT in HDPE using different types of mixing and revulcanization methods. An exciting development in blending is the introduction of thermoplastic elastomers (TPE) based on plastic/rubber blends. The preparation of TPE containing a plastic phase and a highly vulcanized rubber phase, by dynamic vulcanization, has been described.<sup>50-52</sup>

Figure 20 is a plot of the viscosity for 40/60 of HDPE/GRT, HDPE/DGRT, HDPE/RGRT mixed by an internal mixer. This figure clearly indicates that a dynamically cross-linked rubber phase causes an increase in the viscosity of the blends. The melts of thermoplastic elastomer prepared by dynamic vulcanization behave similarly to filled polymer melts.<sup>52</sup> The size, shape, and distribution of the dispersed phase and interfacial adhesion between the two components also affect the flow behavior of polymer blends.

Figure 21 is the plot of tensile strength of HDPE/rubber blends prepared by an internal mixer as a function of HDPE concentration. The tensile strength increases with increasing HDPE loading level. The increase in the tensile strength or Young's modulus is expected as the result of a nature of a plastic phase. The tensile strengths of HDPE/RGRT blends prepared by dynamic revulcanization are better than those of HDPE/GRT or HDPE/DGRT blends. These HDPE/GRT or HDPE/DGRT blends are simply a physical mixture of two incompatible polymers in which a continuous plastic phase is largely responsible for the mechanical properties. In this system, poor adhesion and large particle size are believed to be responsible for the poor pro

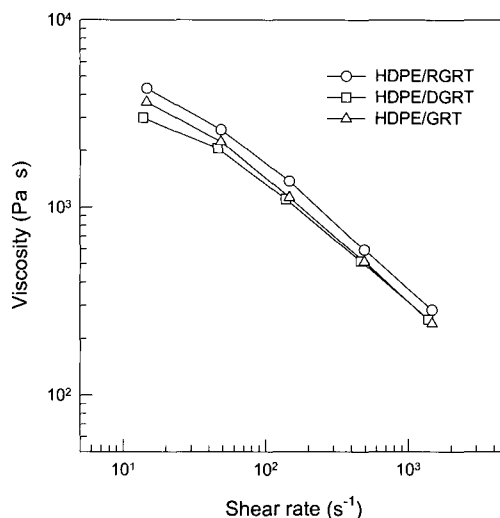


Figure 20. Viscosity vs. shear rate for 40/60 wt. % of HDPE/RGRT, HDPE/DGRT and HDPE/GRT blends.

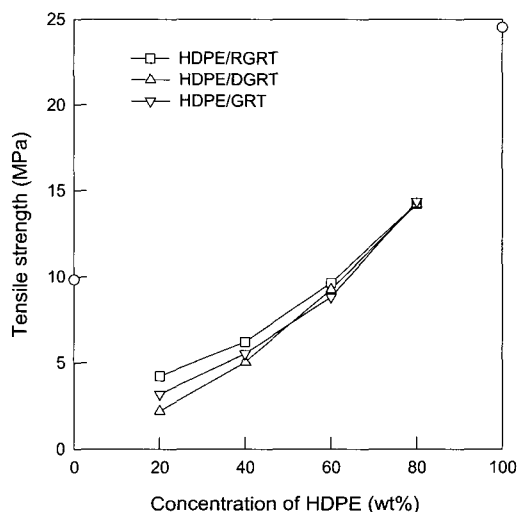
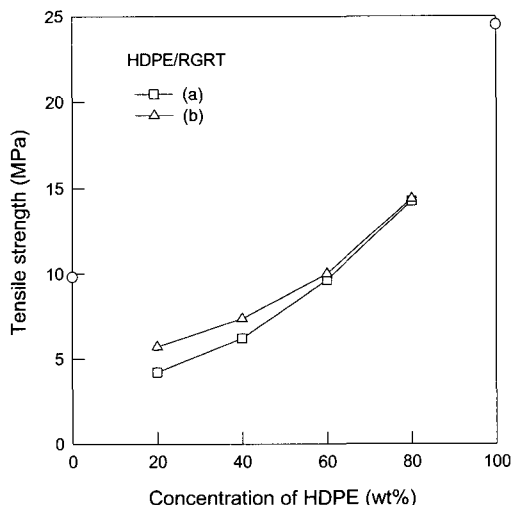


Figure 21. Tensile strength vs. HDPE concentration for HDPE/RGRT, HDPE/DGRT and HDPE/GRT blends; the open circles on the ordinates represent the tensile strength of RGR and HDPE.

erties.<sup>53</sup> In order to get better properties, the particles need to be sufficiently small and adhering to the matrix. On the other hand, the properties of thermoplastic elastomers would be considerably improved if the rubber is partially cross-linked.<sup>54</sup>

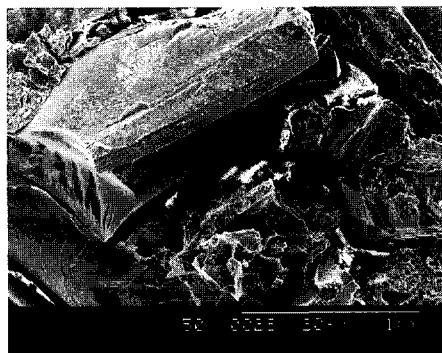
Dynamic cross-linking of thermoplastic elastomers increases the hardness, modulus, strength and recovery properties. Another factor is that certain degree of chemical bonding of the rubber to the plastic is required to improve adhesion between the phases and to better physical properties. As shown in Figure 21, the tensile strength of HDPE/RGRT blends is improved by dynamic revulcanization using a small amount of cross-linking agents.

Figure 22 is a plot of the tensile strength of HDPE/RGRT blends prepared by an internal mixer (a), and mixed by a twin-screw extruder prior to devulcanization and revulcanized in an internal mixer (b). The blend, mixed using a twin-screw extruder prior to devulcanization and devulcanized in the presence of HDPE matrix, has better mechanical properties. This is due to the improved adhesion. Specific reactions between rubber and plastic phases had also occurred during passing blends through the ultrasonic devulcanization reactor.<sup>47,55</sup> Better mechanical properties are believed to be a result of improved adhesion or specific reac-

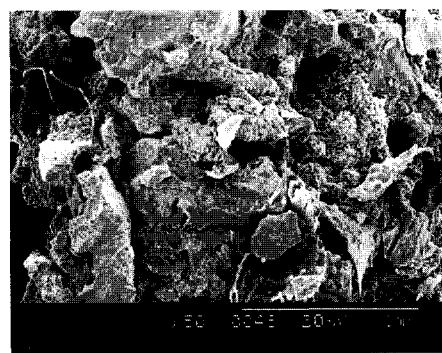


**Figure 22.** Tensile strength vs. HDPE concentration for HDPE/RGRT blends: (a) dynamically revulcanized in an internal mixer, (b) mixed by a twin-screw extruder prior to devulcanization and dynamically revulcanized in an internal mixer.

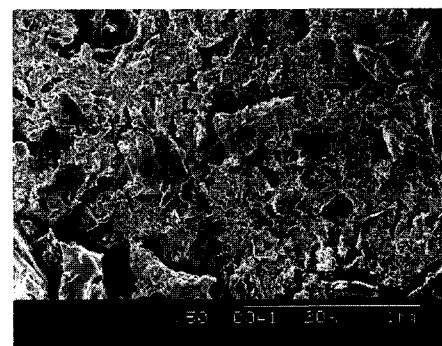
tions between rubber and plastic phase. Generally, the addition of GRT into a thermoplastic polymer matrix results in a significant deterioration in the



(a) HDPE/GRT



(b) HDPE/DGRT



(c) HDPE/RGRT

**Figure 23.** SEM photographs of 20/80 wt. % of HDPE/GRT, HDPE/DGRT and HDPE/RGRT blends.

mechanical properties.<sup>56</sup> Although some applications may tolerate the loss in properties, it is clearly desirable to find methods of overcoming the detrimental effect of the blend. The change in properties depends upon the nature and loading of the GRT, polymer matrix type and adhesion between the GRT and polymer matrixes. For a GRT and plastic matrix, the adhesion or chemical bonding between them is believed to be a major factor controlling the mechanical properties of the composites. In the present study, the passage of the HDPE/GRT blends, mixed by a twin-screw extruder prior to devulcanization, through the devulcanization reactor and subsequent dynamic devulcanization are shown to improve adhesion or chemical reactions between GRT and HDPE.

The morphologies of HDPE/GRT, HDPE/DGRT and HDPE/RGRT blends prepared by an internal mixer are shown in Figure 23. The rubber particles in HDPE/RGRT blends are smaller and more uniform than those in HDPE/GRT or HDPE/DGRT blends. In addition, the rubber particles in HDPE/GRT blends show smooth surfaces. In contrast, the rubber particles in HDPE/RGRT blends indicate rough surfaces with the surface porosity. The dynamic devulcanization of the blends was expected to have significant effects on the wetting characteristics and the interfacial adhesion of the two phases in the blends as they were being mixed. It is quite obvious that the cross-link density of the dispersed rubber phase (Table 4) plays a key role in achieving higher strength. The properties of the blends depend on particle shape, size, and distribution, as well as the interfacial adhesion between the particles and the matrix. The mechanical and rheological properties of the blends depend on the morphologies of blends.

#### IV. Conclusions

The objective of this study is to enhance our understanding of the ultrasonic recycling of rubbers. The effect of pressure and shearing on ultrasonic

process was investigated using a static ultrasonic treatment device. Stronger reductions of cross-link density were observed at a higher pressure, indicating a significant role of pressure in the ultrasonic treatment. Some visible bubbles were observed during the process. Evidently, these bubbles are a proof of the existence of cavitation during the ultrasonic treatment. In static experiment, the unique correlation between gel fraction and cross-link density was shifted toward higher values of cross-link density. Therefore, shearing effect had a significant influence on improving efficiency of ultrasonic treatment.

The ultrasonic treatment of NR/SBR blends was studied with a goal to understand the similarities and differences in the recycling behavior of NR, SBR and their blends. Similar to NR, the ultrasonic power consumption for the blends of 75/25, 50/50 passed through a maximum at 7.5  $\mu\text{m}$ . For SBR and the blend of 25/75, the power consumption increased with increasing ultrasonic amplitude. The higher power consumption led to a higher degree of devulcanization. After the treatment, the cross-link densities of NR/SBR blends were lower than those of NR and SBR possibly due to the reduced degree of unsaturation and chemical reaction during ultrasonic treatment.

The ultrasonic treatment of carbon black filled NR was performed to study the effect of fillers. This experiment indicated a minimum of gel fraction at intermediate amplitude due to the competition between cross-link breakage and reformation during ultrasonic treatment. Carbon black increases the probability of bond scission during ultrasonic treatment, because of the restricted mobility.

The blending devulcanized GRT with HDPE was considered to improve the mechanical properties by dynamic devulcanization of devulcanized GRT in HDPE using different types of mixing methods. The mechanical properties of the blends were improved by dynamic devulcanization. The blends mixed by using the twin-screw extruder prior to devulcanization and devulcanized in the presence of HDPE



matrix were found to have better mechanical properties. This is because specific chemical reactions between rubber and plastic phases were occurred during ultrasonic treatment.

### Acknowledgement

This work was supported by the grants from the National Science Foundation (DMI 9712043) of USA.

### References

1. W. Klingensmith and K. Baranwal, "Recycling of Rubbers: An Overview," *Rubber World*, June, 41 (1998).
2. S. R. Fix, "Microwave Devulcanization of Rubber," *Elastomerics*, 112(6), 38 (1980).
3. P. P. Nicholas, "The Scission of Polysulfide Crosslinks in Scrap Rubber Particles through Phase Transfer Catalysis," *Rubber Chem. Technol.*, 55, 1499 (1982).
4. B. Siuru, "New Technology Recycles Old Tires For New Uses," *Scrap Tire News*, 12(Dec.), 14 (1997).
5. B. Adhikari, D. De and S. Maiti, "Reclamation and Recycling of Waste Rubber," *Prog. Polym. Sci.*, 25, 909 (2000).
6. A. I. Isayev, J. Chen and A. Tukachinsky, "Novel Ultrasonic Technology for Devulcanization of Waste Rubbers," *Rubber Chem. Technol.*, 68, 267 (1995).
7. A. I. Isayev, S. P. Yushmanov, D. Schworm and A. Tukachinsky, "Modeling of Ultrasonic Devulcanization of Tire Rubbers and Comparison with Experiments," *Plastics Rubber Comp. Proc. Appl.*, 25, 1 (1996).
8. A. Tukachinsky, D. Schworm and A. I. Isayev, "Devulcanization of Waste Tire Rubber by Powerful Ultrasound," *Rubber Chem. Technol.*, 69, 92 (1996).
9. M. Tapale and A. I. Isayev, "Continuous Ultrasonic Devulcanization of Unfilled NR Vulcanizates," *J. Appl. Polym. Sci.*, 70, 2007 (1998).
10. A. I. Isayev, S. P. Yushmanov and J. Chen, "Ultrasonic Devulcanization of Rubber Vulcanizates. II. Simulation and Experiment," *J. Appl. Polym. Sci.*, 59, 815 (1996).
11. A. I. Isayev, S. H. Kim and V. Levin, "Superior Mechanical Properties of Reclaimed SBR with Bimodal Network," *Rubber Chem. Technol.*, 70, 194 (1997).
12. S. T. Johnston, J. Massey, E. von Meerwall, S. H. Kim, V. Levin and A. I. Isayev, "Ultrasound Devulcanization of SBR: Molecular Mobility of Gel and Sol," *Rubber Chem. Technol.*, 70, 183 (1997).
13. V. Levin, S. H. Kim, A. I. Isayev, J. Massey and E. von Meerwall, "Ultrasound Devulcanization of Sulfur Vulcanized SBR: Crosslink Density and Molecular Mobility," *Rubber Chem. Technol.*, 69, 104 (1996).
14. V. Levin, S. H. Kim and A. I. Isayev, "Vulcanization of Ultrasonically Devulcanized SBR Elastomers," *Rubber Chem. Technol.*, 70, 120 (1997).
15. V. Levin, S. H. Kim and A. I. Isayev, "Effect of Crosslink Type on the Ultrasound Devulcanization of SBR Vulcanizates," *Rubber Chem. Technol.*, 70, 641 (1997).
16. S. P. Yushmanov, A. I. Isayev and S. H. Kim, "Ultrasonic Devulcanization of SBR Rubber: Experimentation and Modeling Based on Cavitation and Percolation Theories," *Rubber Chem. Technol.*, 71, 168 (1998).
17. J. Yun, A. I. Isayev, S. H. Kim and M. Tapale, "Comparative analysis of ultrasonically devulcanized unfilled SBR, NR and EPDM rubbers," *J. Appl. Polym. Sci.*, 88, 434 (2003).
18. B. Diao, A. I. Isayev, V. Levin and S. H. Kim, "Surface Behavior of Blends of SBR with Ultrasonically Devulcanized Silicon Rubber," *J. Appl. Polym. Sci.*, 69, 2691 (1998).
19. S. E. Shim and A. I. Isayev, "Ultrasonic Devulcanization of Precipitated Silica-Filled Silicone Rubber," *Rubber Chem. Technol.*, 74, 303 (2001).
20. S. E. Shim, S. Ghose and A. I. Isayev, "Formation of Bubbles during Ultrasonic Treatment of Cured Poly (Dimethyl Siloxane)," *Polymer*, 43, 5535 (2002).
21. S. E. Shim, J. Parr, E. von Meerwall and A. I. Isayev, "NMR Relaxation and Pulsed Gradient NMR Diffusion Measurements of Ultrasonically Devulcanized Poly (Dimethyl Siloxane)," *J. Phys. Chem. B*, 106, 12072 (2002).
22. S. Ghose and A. I. Isayev, "Recycling of Unfilled Polyurethane Rubber using High-Power Ultrasound," *J. Appl. Polym. Sci.*, 88, 980 (2003).

23. W. C. Warner, "Methods of Devulcanization," *Rubber Chem. Technol.*, 67, 559 (1994)
24. A. I. Isayev, S. P. Yushmanov and J. Chen, "Ultrasonic Devulcanization of Rubber Vulcanizates. I. Process model," *J. Appl. Polym. Sci.*, 59, 803 (1996).
25. A. I. Kasner and E. A. Meinecke, "Porosity in Rubber, a Review," *Rubber Chem. Technol.*, 69, 424 (1996)
26. A. N. Gent and D. A. Tomkins, "Nucleation and Growth of Gas Bubbles in Elastomers," *J. Appl. Physics*, 40, 2520 (1969).
27. A. N. Gent, "Cavitation in Rubber: A Cautionary Tale," *Rubber Chem. Technol.*, 63, G49 (1990).
28. V. V. Yashin and A. I. Isayev, "A Model for Rubber Degradation under Ultrasonic Treatment: Part II. Rupture of Rubber Network and Comparison with Experiments," *Rubber Chem. Technol.*, 73, 325 (2000).
29. A. J. Kinloch and R. J. Young, "Fracture behavior of polymers," Applied Science Publishers, London, 1983.
30. H. H. Kausch, "Polymer Fracture," Springer-Verlag, Berlin, 1987.
31. V. V. Yashin and A. I. Isayev, "A Model for Rubber Degradation under Ultrasonic Treatment: Part I. Acoustic Cavitation in Viscoelastic Solid," *Rubber Chem. Technol.*, 72, 741 (1999).
32. P. J. Flory and J. Rehner, Jr., "Statistical Mechanics of Cross-Linked Polymer Networks: II. Swelling," *J. Chem. Phys.*, 11, 521 (1943).
33. P. J. Flory, "Statistical Mechanics of Swelling of Network Structures," *J. Chem. Phys.*, 18, 108 (1950).
34. G. Kraus, "Swelling of Filler-Reinforced Vulcanizates," *J. Appl. Polym. Sci.*, 7, 861 (1963).
35. A. I. Isayev, J. Chen and S. P. Yushmanov, in "Simulation of Materials Processing: Theory, Methods and Applications," S. F. Shen and P. Dawson, Eds., Balkema, Rotterdam, 1995.
36. C. K. Hong and A. I. Isayev, "Ultrasonic Devulcanization of Unfilled SBR under Static and Continuous Conditions," *Rubber Chem. Technol.*, 75, 133 (2002).
37. S. D. Lubetkin, in "Controlled Particle, Droplet and Bubble Formation," Chap. 6, edited by D. Wedlock, Butterworth-Heinemann Ltd., Oxford, 1994.
38. H. Kwak and R. Panton, "Gas Bubble Formation in Non-Equilibrium Water Gas Solutions," *J. Chem. Phys.*, 78(9), 5795 (1983).
39. D. Niyogi, R. Kumar and K. Gandhi, "Modeling of Bubble-Size Distribution in Free Rise Polyurethane Foams," *AIChE J.*, 38(8), 1170 (1992).
40. J. Han and C. D. Han, "Bubble Nucleation in Polymeric Liquids. 2. Theoretical Considerations," *J. Polym. Sci.: Part B: Polym. Phys.*, 28, 743 (1990).
41. L. E. Kinsler, A. Frey, A. Coppers and J. Sanders, "Fundamentals of Acoustics," Wiley, NY, 1982.
42. J. O. Hirschfelder, C. Curtis and R. Bird, "Molecular Theory of Gases and Liquids," Wiley, NY, 1954.
43. J. Brandrup and H. Immergut, ed., "Polymer Handbook," 3rd ed., Wiley, NY, 1989.
44. A. J. Tinker and K. P. Jones, "Blends of Natural Rubber," Chapman & Hall, NY, 1998.
45. C. K. Hong and A. I. Isayev, "Continuous Ultrasonic Devulcanization of Carbon Black-Filled NR Vulcanizates," *J. Appl. Polym. Sci.*, 79, 2340 (2001).
46. C. K. Hong and A. I. Isayev, "Continuous Ultrasonic Devulcanization of NR/SBR Blends," *J. Appl. Polym. Sci.*, 83, 160 (2002).
47. A. I. Isayev and C. K. Hong, "Novel Ultrasonic Process for in-situ Copolymer Formation and Compatibilization of Immiscible Polymers," *Polym. Eng. Sci.*, 43(1), 91 (2003).
48. S. Wolf and M. J. Wang, in "Carbon Black," Ed., J. B. Donnet, R. C. Bansal and M. J. Wang, Chap. 9, Science and Technology, NY, 1993.
49. L. Bateman, "The Chemistry and Physics of Rubber-like Substance," Wiley, NY, 1963.
50. A. Y. Coran and R. Patel, "Rubber-Thermoplastic Compositions. 1. EPDM-Polyethylene Thermoplastic Vulcanizates," *Rubber Chem. Technol.*, 53, 141 (1980).
51. F. Cai and A. I. Isayev, "Dynamic Vulcanization of Thermoplastic Copolyester Elastomer Nitrile Rubber Alloys. 1. Various Mixing Methods," *J. Elast. Plast.*, 25, 74 (1993).
52. F. Cai and A. I. Isayev, "Dynamic Vulcanization of Thermoplastic Copolyester Elastomer Nitrile Rubber Alloys. 2. Rheology, Morphology and Properties," *J. Elast. Plast.*, 25, 249 (1993).
53. C. K. Hong and A. I. Isayev, "Blends of Ultrasonically Devulcanized and Virgin Carbon Black Filled NR," *J. Mater. Sci.*, 37, 385 (2002).
54. S. K. De and A. K. Bhowmick Eds, "Thermoplastic Elastomers from Rubber-Plastic Blends," Ellis Horwood, NY, 1990.

55. C. K. Hong and A. I. Isayev, "Plastic/Rubber Blends of Ultrasonically Devulcanized GRT with HDPE," *J. Elast. Plast.*, 33, 47 (2001).
56. P. K. Pramanik and W. E. Baker, "Toughening of Ground Rubber Tire Filled Thermoplastic Compounds Using Different Compatibilizer Systems," *Plast. Rubb. Comp. Proc. Appl.*, 24(4), 229 (1995).